(23) Crothers, D.; Kallenbach, N. *J. Chem. Phys.* **1966**, *45*, 917.
(24) Poland, D.; Scheraga, H. A. "Theory of Helix–Coil Transitions in Biopolymers"; Academic Press: New York, 1970.
(25) Mattice, W. L.; Skolnick, J. *Macromolecules* **1982**, *15*, 1088.
(26) Mattice, W. L.; Srinivasan, G.; Santiago, G. *Macromolecules* **1980**, *13*, 1254.
(27) Maroun, R.; Mattice, W. *Biochim. Biophys. Acta* **1984**, *784*, 133.
(28) Ihara, S.; Ooi, T.; Takahashi, S. *Biopolymers* **1982**, *21*, 131.
(29) Mayer, J.; Mayer, M. "Statistical Mechanics"; Wiley: New York, 1940; pp 213–217.
(30) Hodges, R.; Saund, A.; Chong, P.; St. Pierre, S.; Reid, R. *J. Biol. Chem.* **1981**, *256*, 1214.
(31) Flory, P. "Statistical Mechanics of Chain Molecules"; Wiley: New York, 1969; p 251.
(32) Schultz, G.; Schirmer, R. "Principles of Protein Structure"; Springer-Verlag: New York, 1979.
(33) Holtzer, M.; Holtzer, A. *Macromolecules* **1972**, *5*, 294.
(34) Skolnick, J. *Macromolecules*, in press.
(35) Skolnick, J.; Holtzer, A., unpublished results.
(36) Krishnan, K. S.; Brandts, J. F.; Lehrer, S. *FEBS Lett.* **1978**, *91*, 206.
(37) Holtzer, M. E.; Holtzer, A.; Skolnick, J. *Macromolecules* **1983**, *16*, 173.
(38) Pato, M.; Mak, A.; Smillie, L. *J. Biol. Chem.* **1981**, *256*, 593.
(39) Williams, D. L., Jr.; Swenson, C. *Biochemistry* **1981**, *20*, 3856.
(40) Potekhin, S.; Privalov, P. *J. Mol. Biol.* **1982**, *159*, 519.
(41) Betteridge, D.; Lehrer, S. *J. Mol. Biol.* **1983**, *167*, 481.
(42) Holtzer, M. E.; Holtzer, A.; Skolnick, J. *Macromolecules* **1983**, *16*, 462.
(43) Chao, Y. Y. H.; Holtzer, A. *Biochemistry* **1975**, *14*, 2164.
(44) Graceffa, P.; Lehrer, S. *Biochemistry* **1984**, *22*, 2606.
(45) Skolnick, J.; Holtzer, A. *Macromolecules* **1982**, *15*, 812.
(46) Skolnick, J. *Macromolecules*, submitted.

Theory of α-Helix-to-Random-Coil Transition of Two-Chain, Coiled Coils. Application of the Augmented Theory to Thermal Denaturation of α-Tropomyosin

Jeffrey Skolnick† and Alfred Holtzer*

Department of Chemistry, Washington University, St. Louis, Missouri 63130.
Received November 21, 1984

ABSTRACT: The statistical mechanical theory of the helix-to-random-coil transition in two-chain, α-helical coiled coils has recently been augmented by inclusion of the effects of loop entropy and out-of-register ("mismatched") structures. This theory is applied to experimental data on non-cross-linked α-tropomyosin at nearly neutral and at acidic pH, using extant values of helix initiation (σ) and propagation (s) parameters for each amino acid in the sequence. A semiquantitative fit of the helix content (from circular dichroism measurements) vs. temperature (0–80 °C) is obtained at each pH, covering a 1000-fold range of protein concentration. The algorithms for the mean interhelix interaction free energy per mole of turn pairs (RT ln $w(T)$) needed to produce the fit at each pH provide curves of RT ln $w(T)$ vs. T that are similar in range and in shape, each showing a minimum near room temperature. Theory is also compared with independent experiments, in particular light scattering and cross-linkability studies at nearly neutral pH. The temperature dependence of the weight-average molecular weight at nearly neutral pH, as recently determined by light scattering, agrees well with the theoretical prediction. The observed high degree of cross-linkability of tropomyosin in the native state can be reconciled with the theoretically calculated fraction of in-register molecules under the benign conditions of the cross-linking experiments. Examination shows that the principal cause of the greater stability of α-tropomyosin at low pH lies in the augmented short-range (σ,s) interactions of aspartic and glutamic residues over those of the aspartate and glutamate species which predominate near neutral pH. In fact, it is shown that, with small adjustment (within experimental error) in these parameters, the same interhelix interaction free energy algorithm can be used to explain the full range of data at both pHs. A discussion of the implications of this result is given, wherein it is shown that the interhelix salt bridges, while they may provide enough free energy at nearly neutral pH to ensure that the helices associate in parallel, make a contribution to the total interhelix interaction that is relatively small compared with the hydrophobic contribution. The statistical theory developed here is compared with the all-or-none-stages model brought forward elsewhere; it is suggested that the latter disagrees with the recent light scattering data and is difficult to reconcile with accepted ideas concerning loop entropy.

I. Introduction

The native tropomyosin molecule is a two-chain, α-helical, coiled coil.[1] That is, the accepted picture of the molecule is that it comprises two essentially completely α-helical polypeptide chains arranged side-by-side, in parallel and in register, and given a slight supertwist.[2-8] The simplicity of this structure makes it an attractive object of study as much for its relevance to the larger problem of protein conformational stability as for its inherent interest in the biochemistry of muscle.[9-14] Here is a fully functional protein that has only one type of secondary structure (α-helix), no tertiary structure (i.e., no folding of a given chain back upon itself), and a quaternary structure that allows chain–chain interactions only in a fixed, repetitive geometrical context. The molecule thus forms a natural model system for the problem of sorting out "short-range" and "long-range" contributions to the conformational stability of protein structures and their relationship to the primary structure.

Determination and study of the primary structure of tropomyosin have clarified, at least in a qualitative way, some aspects of the array of stabilizing forces.[15-17] The amino acid sequence in each 284-residue chain is based on a pseudo-repeating heptet (denoted by letters a–g) in which the first and fourth residues (a, d) are obligatory hydrophobes, the fifth (e) bears an obligatory negative charge, and the seventh (g) bears an obligatory positive charge. When such a chain is coiled into a right-handed α-helix, the resulting structure is locally highly amphipathic; the obligatory hydrophobes appear on one face of the resulting molecular cylinder, while a line of positive charge appears

† Alfred P. Sloan Foundation Fellow.

0024-9297/85/2218-1549$01.50/0 © 1985 American Chemical Society

on one side of them and a line of negative charge on the other. These lines of hydrophobes and charges are not quite parallel to the helix axis but trace a gentle, left-handed helix of a pitch corresponding to the supertwist. It seems clear that two such α-helical chains pack into the parallel, closely registered coiled coil because of a combination of favorable hydrophobic and electrostatic interactions. The chains are closely in register because appreciable staggering would expose hydrophobes to the aqueous medium.[9,18] They are in parallel because an antiparallel arrangement, while it could satisfy the hydrophobes, would place the "line" of positive charges adjacent to the similar line on the second chain and would do the same for the negative charges.[18,19]

The simplicity of the structure makes it susceptible to treatment by statistical mechanics. In a series of papers, such a theory was developed[10] and applied to a small (43 residues/chain) synthetic analogue,[11] to α-tropomyosin (molecules of which have two α-chains, an α-chain being one of two genetic variant chains, α and β, that have been sequenced),[12,13] and to two enzymic fragments of α-tropomyosin.[14] This theory is very much in the spirit of the earlier theory of Zimm and Bragg[20] and of Nagai[21] for the helix–coil transition in single-chain polypeptides. In the single-chain theory, the relevant short-range interactions responsible for helix stability are embodied in two parameters: a helix initiation parameter (σ) and a helix propagation parameter (s), defined so that the standard free energy change in converting a randomly coiled chain to one with a total of n_h helical residues in ν helical runs is $-kT \ln (\sigma^{\nu} s^{n_h})$. This theory has been very successful in explaining what is known about the helix–coil transition in single-chain polypeptides.[22] An enormous body of data exists providing values of σ and $s(T)$ for essentially all the amino acid residue types found in proteins.[23-38]

In extending this theory to two-chain molecules, we introduced an additional parameter (which we now call w°) to embody the helix–helix interchain interactions of the coiled-coil structure.[10] A given heptet was divided into two blocks, a four-residue block (a–d) and a three-residue block (e–g). A block is thus very nearly one α-helical turn. The four-residue block on one helical chain has two obligatory hydroprobes (a, d) that can interact favorably with hydrophobes on the adjacent helical chain. The three-residue block has one positively charged (g) and one negatively charged (e) group that can interact favorably with their oppositely charged neighbors on the adjacent chain, provided the chains are juxtaposed in parallel. The standard free energy for bringing two widely separated, positionally (rotationally and translationally) fixed helical blocks together to form a pair of interacting, positionally fixed helical blocks is written $-kT \ln w^\circ(T)$.

To realize the theory, the independently determined experimental values of σ and $s(T)$ appropriate to each amino acid residue in the sequence were employed. However, no analogous, independent data exist that establish values of $w^\circ(T)$ for a given interacting hydrophobic or electrostatic pair of residues. Hence, the experimental helix content at each temperature T was used with the theory to establish a mean value of $w^\circ(T)$ at that temperature.[11-14] Thus, the $w^\circ(T)$ values obtained make no distinction between hydrophobically and electrostatically interacting blocks or between one hydrophobic or electrostatic residue type and another. This crudity is not inherent in the theory, which is capable of handling the full complexity of interactions, but is simply a result of our present ignorance in quantitating hydrophobic and electrostatic interactions. The realized theory served to fit the data, provided molecular interpretations of many known facts about the helix–coil transition in tropomyosin, and nowhere disagreed with experiment significantly enough so as to compel its rejection.

Recently, the theory has been augmented in two very important respects.[39-41] First, the effects of loop entropy were included. In the original theory, loop entropy was explicitly excluded from consideration. In a subsequent, more penetrating analysis of the problem, it was shown theoretically that this effect is, in fact, rather important.[39] Indeed, it serves to eliminate configurations in which randomly coiled residues form a closed loop, because of the marked reduction of conformational entropy they experience. Thus, molecular states in which the two chains display two interacting double-helical stretches separated by a randomly coiled stretch (which constitutes the loop) are extremely unlikely. This effect significantly changes the weighting of the various states. Second, the original theory explicitly excluded out-of-register ("mismatched") states, i.e., those in which, say, the nth block on one chain might be helical and interact not with the nth block on the other chain but with some other helical block on the other chain. Subsequent development of the theory showed that such "mismatched" states also make a significant contribution.[41]

It is our present purpose to apply this greatly augmented theory to data on α-tropomyosin at both neutral and acidic pH. In the interim, additional experimental results have become available that are appropriate to the purpose: circular dichroism (CD) data that extend the temperature range of the neutral solution measurements originally employed in the theory[42] and light scattering data, obtained to test predictions of the original theory concerning the extent of chain dissociation accompanying the transition.[43] However, implementation of the augmented theory still requires use of a helix–helix interaction parameter that is averaged over the entire molecule, blurring possible distinctions between hydrophobic and electrostatic interactions and among the various possible pairs of species of hydrophobic and electrostatic contacts. Thus, the helix–helix interaction parameter at a given T is still obtained by trial until a value is obtained that, using the augmented theory, fits the experimental (CD) helix content at the temperature. This value is refered to as $w(T)$ to distinguish it from the corresponding quantity (now called $w^\circ(T)$) determined with the original theory. Furthermore, in the augmented theory employed here, a mismatched conformation is only counted if it is out of register by an even number of blocks; i.e., it is assumed that electrostatic block to hydrophobic block contacts are inherently unstable and do not contribute. It is also assumed throughout that antiparallel states do not contribute.

As will be seen, most of the results obtained with the augmented theory are qualitatively, sometimes even semiquantitatively, in agreement with those obtained with the simpler theory. Moreover, we still find no disagreement compelling rejection of the theory; quite the contrary, some major qualitative features of the helix–coil transition in tropomyosin, including ones inexplicable before any two-chain theory was available, become intelligible in the light of the theory, and new predictions are generated that, now or in the future, may be compared with experiment. Finally, it is possible to examine other extant models of the transition critically from the statistical mechanical viewpoint provided by the augmented theory.

II. Methods

Consider the dimerization reaction of two, identical, single-chain polypeptides capable of associating through

helix–helix interactions to form two-chain species:

$$A + A \rightleftarrows A_2 \quad (1)$$

Defining C_0 as the total concentration of protein in formula weights of chains per liter of solution, (A) as the molar concentration of single chains (monomers), and (A_2) as the molar concentration of two-chain molecules (dimers), then

$$C_0 = (A) + 2(A_2) \quad (2)$$

Furthermore, the equilibrium constant K for association may be written as

$$K = (A_2)/(A)^2 = (1 - g_m)/(2g_m^2C_0) \quad (3)$$

wherein g_m is the weight fraction of chains that are dissociated, i.e., exist in solution as single strands. Equation 3 may be solved for g_m to give

$$g_m = \frac{-1 + (1 + 8KC_0)^{1/2}}{4KC_0} \quad (4)$$

Following our previous method,[10] the experimentally observed circular dichroism can be related to overall helix fraction of the solution Φ_h, which in turn is related to the helix fraction of the monomer f_{hm} and of the dimer f_{hd} via

$$\Phi_h = g_m f_{hm} + (1 - g_m) f_{hd} \quad (5)$$

We next represent the above phenomenological quantities by their appropriate statistical mechanical expressions.

It is a well-known result of statistical mechanics that the equilibrium constant K for the dimerization reaction of eq 1 is related to the partition function of the dimer Z_d and monomer Z_m by[44]

$$K = VZ_d/Z_m^2 \quad (6)$$

wherein V is the volume of the system. The partition function of the monomer is obtained from eq II-9 of ref 40. Proceeding by analogy to Zimm's treatment of the helix–coil transition in DNA,[45] we write for Z_d

$$Z_d = (u/V)Z_{int} \quad (7)$$

in which Z_{int} is the internal partition function of the dimer and u is the product of three factors: (a) the volume of configuration space accessible to the center of mass of one α-helical turn in the dimer when the α-helical turn in the other chain is held positionally fixed; (b) an orientational factor β that accounts for the relative allowed angular orientation of the α-helical turns that permit the interhelical interaction to occur; (c) the ratio γ of the volume of configurational space spanned by the internal degrees of freedom of the α-helical turn in the dimer to that in the monomers. Following Mayer and Mayer,[44] we shall write

$$u = \beta\gamma\pi h(d_{max}^2 - d_{min}^2) \quad (8)$$

To implement eq 8, we substitue for h the length of the α-helical turn, 5.4 Å, for d_{min}, the distance of closest approach, 7.0 Å,[46] and for d_{max}, 14 Å, a value obtained from d_{min} by adding an amount suggested by recent X-ray crystallographic data.[47] Unfortunately, neither β nor γ is well-known, but clearly each is less than unity. We have somewhat arbitrarily set $\beta\gamma = 0.144$, which provides u equal to 359 Å,[3] which is numerically the same as the excluded volume of the two backbone helix disks, the value previously, and somewhat naively, employed.[10] This value of $\beta\gamma$ lies approximately midway between a maximum of unity and a minimum estimated to be on the order of 0.002, the latter obtained by assuming a maximum angle of 10° between the principal axes of the two helical turns and an allowed azimuthal angular range of contact of 100°. As discussed below, our results are insensitive to the particular value of u chosen, provided that u lies within the physically reasonable range.

The internal partition function of the dimer, Z_{int}, sums over all states that contain at least one interacting pair of α-helical turns, and for a dimer composed of N_B α-helical turns ("blocks") is given by

$$Z_{int} = (2 - \delta_{N_B,N}) \sum_{N=1}^{N_B}{}' Z(N) \quad (9)$$

wherein $\delta_{N_B,N}$ is the Kronecker delta and the prime indicates a sum over odd N only. That is, we exclude charge–hydrophobe contacts in the quasi-repeating heptet, summing only over all in- and out-of-register states wherein only hydrophobic–hydrophobic contacts and attractive charge–charge contacts are allowed in block–block interactions. $Z(N)$ is the contribution to the partition function of all those states that are $N_B - N$ blocks out of register. $Z(N)$ may be calculated via eq II-2a ref 41.

It should be pointed out that previously[41] we incorrectly included the possibility of all random-coil states in the calculation of the internal partition function of the dimer. Thus, the expression $2Z_m - 1$ in eq II-1 of ref 41 for the internal partition function (denoted there by Z_{sd}) should be deleted. Finally, the fraction of molecules that are $N_B - N$ blocks out of register is given by

$$P(N) = (2 - \delta_{N_B,N})Z(N)/Z_{int} \quad (10)$$

Equation 5 expresses the overall helix content of the solution Φ_h in terms of g_m, f_{hm}, and f_{hd}. The value of g_m follows from eq 4, f_{hm} is obtained from eq II-12 of ref 40, and f_{hd} is calculated by employing eq II-11 of ref 41 but with the superfluous term $f_{hm}Z_m/Z_{sd}$ deleted.

To realize these theoretical equations, values of $s(T)$ for each amino acid residue were obtained from algorithms chosen to fit the experimental values determined in Scheraga's laboratory.[23-38] Values of σ were obtained from the same source. These algorithms have been previously reported, including updated values for isoleucine and glutamine.[11,12] Algorithms for $s(T)$ and values for σ appropriate to aspartic and glutamic acid residues at acidic pH were also as previously presented.[13]

The data used for α-tropomyosin at pH 7 were values picked off spline curves of helix content vs. T (at each of three protein concentrations) drawn through the values recently reported.[42] These data span a more than 1000-fold range of protein concentration. The aqueous medium contained 0.500 M NaCl, 50 mM NaP_i, and 1.0 mM DTT. The resulting smoothed values differ only slightly from those used earlier. The values differ mainly because the new data cover a wider temperature range, necessitating slight shifts in the spline curves, but also because of interim recalibration of the CD spectrometer.

To obtain values of $w(T)$, trial values were inserted into the theory until the calculated value of overall helix content (Φ_h) matched the experimental value. This procedure was carried out for ten temperatures at each protein concentration (30 points in all near neutral pH). As in earlier work,[12,13] points were accepted only between 15% and 93% helix, because of the extreme sensitivity of w to slight changes in Φ_h outside that range. These values of $w(T)$ were fit, as before, to the equation

$$-\Delta G^\infty = RT \ln w = BT \ln T + A_0 + A_1T + A_2T^2 \quad (11)$$

but the quadratic term was included only if it resulted in a material improvement in the fit. This "best" algorithm for the negative free energy of helix-block to helix-block interchain interaction was then used in the theoretical equations to generate theoretical values for desired properties.

Table I
Coefficients for RT ln $w(T)$ Algorithms[a]

algorithm	B	A_0	A_1	A_2
RT ln $w(T,7)$	52.627 425 9	15 793.499 8	−351.163 555	
RT ln $w(T,2)$	126.821 470	38 469.517 6	−850.102 690	
RT ln $w(T,2ad)$	106.515 130	32 497.274 7	−714.312 522	
RT ln $w(T,7/2ad)$	−495.091 665	−66 146.377 2	2772.287 76	0.912 581 315

[a] RT ln $w = BT$ ln $T + A_0 + A_1T + A_2T^2$, cal·(mol of block pairs)$^{-1}$.

The data used for α-tropomyosin at acidic pH were essentially those given previously,[13] but adjusted slightly to compensate for small interim changes in absolute instrumental calibration. This small ajustment makes them more closely comparable to the new values for the pH 7 data, but no change in any conclusion results from this adjustment. The aqueous medium contained 0.59 M NaCl, 0.01 M HCl, and 0.5 M DTT. The procedures for obtaining $w(T)$ for the acidic solutions were the same as for the nearly neutral case except that somewhat fewer points were employed. This is justified because, in the accessible temperature range (i.e., where Φ_h (T, pH 2) is between 0.15 and 0.93), RT ln w is monotonic and easier to characterize at pH 2.

III. Theoretical Results

A. Non-Cross-Linked α-Tropomyosin Near Neutral pH. Values of the intramolecular interhelix interaction required to fit the experimental fraction helix at pH 7.4 are shown in Figure 1A as RT ln w vs. temperature. The curve computer-fit to eq 11 with these values is also shown and is seen to fit the points rather well. In the following, we will refer to values of the ordinate given by this algorithm as RT ln $w(T,7)$, reflecting the fact that it is based on values of the parameter w chosen to fit the experimental helix content at temperature T near neutral pH. Numerical values for the coefficients of eq 11 corresponding to this curve are given in Table I.

Because of the paucity of points near and below the temperature of the minimum in the curve, it is legitimate to ask if the shape is actually an artifact of the curve-fitting procedure or is required by the data. A slightly curved line declining steadily to ~440 cal·(mol of block pairs)$^{-1}$ on the ordinate axis as temperature drops would fit the points almost as well. However, such an algorithm would predict a helix content of ~48% at 0 °C, far below the experimental value of over 95%. Indeed, even if the curve is allowed to level off at lower temperatures bringing it to, say, 475 cal·(mol of block pairs)$^{-1}$ at 0 °C, this still provides a helix content at that temperature of barely 90%, still well below the experimental value. The minimum seems to be real, although its exact position and depth are less certain. The overall shape is similar to that obtained when the simpler theory is used.[12]

Using the RT ln $w(T,7)$ algorithm in the new theory, along with the experimental array of σ and $s(T)$ values appropriate to neutral pH, allows calculation of such properties as the fraction helix, $\Phi_h[\sigma(7),s(T,7),w(T,7)]$, as a function of temperature at various concentrations of protein. Such curves are displayed along with smoothed experimental data points on Figure 1B for the two concentrations at the extremes of the data range. These theoretical curves fit the data tolerably well, about as well as the simpler, earlier theory. At these extreme concentrations, the theory mimics the data semiquantitatively; at the median concentration (not shown), the fit is essentially quantitative.

The theoretical curve for the helix content of dimer (two chain) molecules is also shown in Figure 1B (dashed curve). It is an important prediction of the theory that the helix content of dimer species is always greater, and at higher temperatures appreciably greater, than that of the entire solution, reflecting the low helix content and increasing fraction of monomer species (dot–dash curve). Thus, the theory insists that the chain dissociation and loss of helix content go hand in hand.

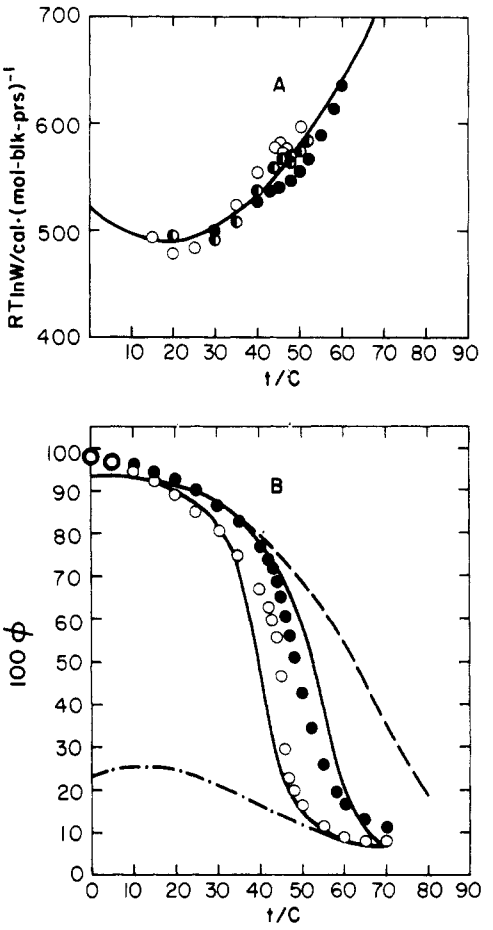

Figure 1. (A) RT ln w vs. temperature for non-cross-linked α-tropomyosin at pH 7.4: open circles, 0.0044 mg·cm^{-3}; half-filled circles, 0.104 mg·cm^{-3}; filled circles, 5.2 mg·cm^{-3}. Solid curve is RT ln $w(T,7)$ algorithm. (B) Percent helix vs. temperature for non-cross-linked α-tropomyosin at pH 7.4: open circles, smoothed data for 0.0044 mg·cm^{-3}; filled circles, smoothed data for 5.2 mg·cm^{-3}. Solid curves are from theory using RT ln $w(T,7)$ algorithm (i.e., curves are $\Phi_h[\sigma(7),s(T,7),w(T,7)]$) for the same concentrations. Dashed curve is from theory for dimer species, using same algorithm. Dot–dash curve is from theory for single chains at pH 7.4.

B. Non-Cross-Linked α-Tropomyosin at Acidic pH. Values obtained from the theory to fit the data at pH 2 are shown in Figure 2A, along with the computer-fit curve. The latter provides an algorithm to calculate RT ln $w(T,2)$; its numerical coefficients are also given in Table I. The algorithm is seen to fit the points almost perfectly and can be used in the theory in conjunction with the other parameters appropriate to pH 2 (i.e., $\sigma(2)$ and $s(T,2)$) to calculate fraction helix, $\Phi_h[\sigma(2),s(T,2),w(T,2)]$. The results are shown in Figure 2B as solid curves along with the data.

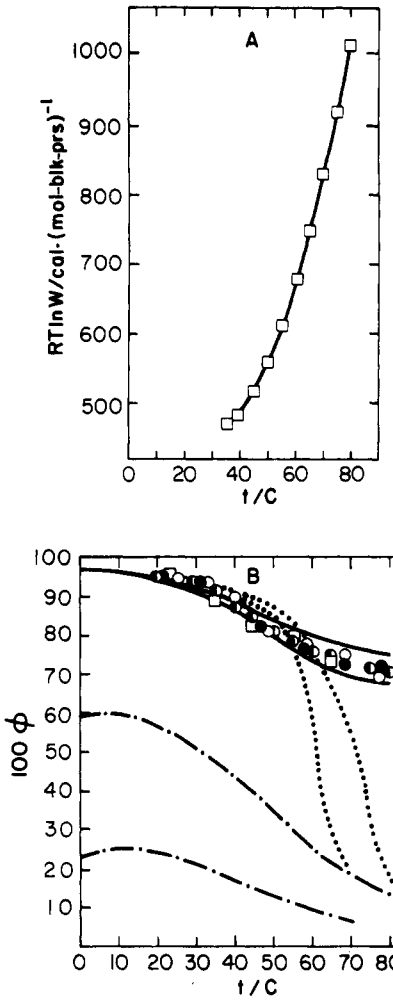

Figure 2. (A) RT ln w vs. temperature for non-cross-linked α-tropomyosin at pH 2: open squares, 0.0058 mg·cm^{-3}. Solid curve is RT ln $w(T,2)$ algorithm. (B) Percent helix vs. temperature for non-cross-linked α-tropomyosin at pH 2: open circles, open squares, open triangles, and filled circles are data for respectively 0.0051, 0.0058, 0.120, and 5.2 mg·cm^{-3}. Solid curves are from theory using RT ln $w(T,2)$ algorithm (i.e., curves are $\Phi_h[\sigma(2),s(T,2),w(T,2)]$) for 0.0058 (lower curve) and 5.2 (upper curve) mg·cm^{-3}. Dotted curves are from theory using RT ln $w(T,7)$ algorithm (i.e., curves are $\Phi_h[\sigma(2),s(T,2),w(T,7)]$) for the same two concentrations. Dot–dash curves are from theory for single chains at pH 2 (upper) and pH 7.4 (lower).

The curves mimic the experiments virtually quantitatively. In particular, although they predict a small dependence on protein concentration in the relevant range, the difference is too small to be reliably detected. One of the principal experimental findings at pH 2 is that, unlike pH 7.4, there is essentially no dependence of helix content of protein concentration in the accessible range. The theory shows the same thing. The algorithms obtained from the data sets at neutral and at acidic pH are not the same. This difference is discussed below along with other matters.

IV. Discussion

A. Comparison of Theory with Extrinsic Experiments. We have seen that the theory provides an acceptable fit to the fraction helix vs. temperature curves obtained from CD measurements. However, the very same measurements were used to obtain the algorithm for RT ln $w(T)$ vs. T that is required to realize the theory. Thus, agreement merely signifies that the theory is self-consistent, not that it is correct. To obtain evidence on the latter point, theory must be compared with experiments that are independent of those employed in realizing the theory itself, i.e., with "extrinsic" experiments. In this section we compare theory with two such experiments: light scattering and cross-linkability studies.

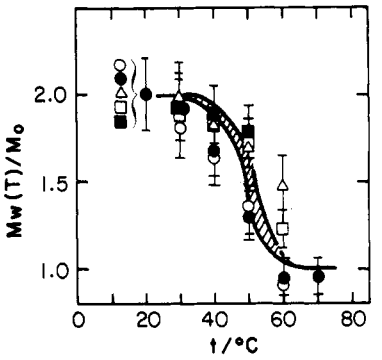

Figure 3. Weight-average aggregation number (M_w/M_0, with M_0 equal to the chain molar mass) vs. temperature at pH 7.4. Points are experimental values: blocked tropomyosin at 0.33 (open circles) and 0.56 (filled circles) mg·cm^{-3}; reduced tropomyosin at 0.33 (open squares), 0.85 (open triangles), and 0.99 (filled squares) mg·cm^{-3}. Band covers range of values calculated for 0.33–0.99 mg·cm^{-3} from theory using RT ln $w(T,7)$ algorithm.

Recently, in response to the challenge put forward by the earlier theory, light scattering measurements were reported on α-tropomyosin as a function of temperature, thus providing $M_w(T)$, the weight-average molecular weight, vs. T.[43] For technical reasons, these data were taken in the protein concentration range ~0.3–1.2 mg·cm^{-3}. This is within the range of our CD data (0.0044–5.2 mg·cm^{-3}). Given the RT ln $w(T)$ algorithm, the theory can be used to calculate relevant properties at any protein concentration selected. From the calculated dimer and monomer populations, the weight-average molecular weight is easily obtained. These theoretical values were calculated with the new theory for the two extreme protein concentrations of the light scattering data. The entire range of the results is given as the hatched band on Figure 3. The light scattering experimental points are also shown.

Comparison of the theoretical prediction with the experiment shows agreement within the unavoidably substantial experimental error of the light scattering data. It seems to us that this represents an important verification of the statistical picture of the transition. As noted above, in that picture, chain dissociation plays a vital role in the loss of helix in the principal transition. This conclusion from theory cannot be tested directly, because at benign temperatures the system dimerizes quantitatively. The light scattering experiments support the idea that dissociation and the helix–coil transition are concurrent events. This is contrary to extant views in which dissociation is supposed to occur rather further along in the transition, after most of the helix content has been lost.[48,49] The light scattering results make this latter view untenable.

We turn next to experiments on cross-linkability. These show plainly that near room temperature at least 90% of the tropomyosin molecules are disulfide cross-linkable by a reaction taking at most a few hours.[50] This is true not only of native tropomyosin but also of tropomyosin that has been denatured and then renatured.[51] The accepted interpretation of these results is that the equilibrium state of the tropomyosin molecule consists of two chains in parallel and essentially in register, for otherwise a sulfhydryl at Cys-190 could not reach its counterpart on the adjacent chain.

The present theory allows out-of-register structures and therefore can be used to calculate their equilibrium populations. The results are shown on Figure 4 as the percent of dimer molecules (at 20 °C, the temperature of cross-

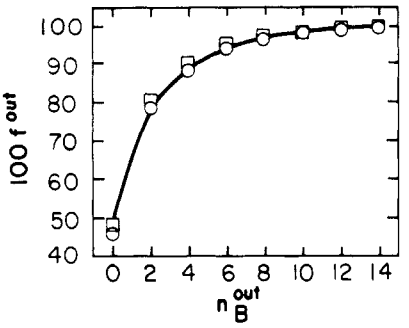

Figure 4. Out-of-register populations at pH 7 and 20 °C. Ordinate is percent of molecules out of register by n_B^{out} blocks or less. Abscissa is n_B^{out}. Points are from theory using RT ln $w(T,7)$ algorithm (open circles) or RT ln $w(T,7/2ad)$ algorithm (open squares).

linking) that are out of register by at most n_B^{out} helical blocks vs. n_B^{out}. Keep in mind that one block $\simeq$ one helical turn and that molecules cannot be mismatched by an odd number of blocks. Figure 4 shows that nearly 50% of the molecules are predicted to be *exactly* in register and therefore unquestionably cross-linkable. Moreover, ~80% of the molecules are within two helical turns of exact register. Thus, the theory, even in its narrowest interpretation as a set of equilibrium states, explains most of the cross-linkability observed by experiment.

Moreover, if one recognizes that thermal agitation is bound to produce some freedom of motion, it is very easy to see how the total cross-linkability could be raised to 90% of the molecules. It is known that the intact coiled coil does not possess sufficient freedom for helices to exchange (by dissociation–reassociation or whatever) from molecule to molecule on the normal experimental time scale (<1 week).[51] However, the motions required here would need to cover a distance of only two helical turns (~10 Å) to produce the experimental cross-linkability. X-ray studies of tropomyosin indicate root-mean-square excursions of ~8 Å for the Cys-190 region of the molecule at 20 °C.[47] Segments conceivably could spend as much as 25% of the time ~10 Å from their average position. It seems likely therefore that helices may loosen enough locally for long enough to reach one heptet away and cross-link. Alternatively, helix "skittering" or reptation could convert in-register molecules to two-blocks-out-of-register molecules and vice versa in a dynamic equilibrium. Theory thus can rationalize the substantial cross-linkability found experimentally.

B. Combined Algorithm for Data at Nearly Neutral and at Acidic pH. Comparison of different algorithms for RT ln $w(T)$ is facilitated by examination of Figure 5. On Figure 5A, the algorithm derived from the CD data at near-neutral pH, i.e., RT ln $w(T,7)$, is shown as the dotted curve, while that derived from CD data at acidic pH, i.e., RT ln $w(T,2)$, is shown as the dot–dash curve. The solid and dashed curves are discussed below. Figures 5B, 6A, and 6B display the corresponding $\Delta\bar{H}^\infty$, $\Delta\bar{S}^\infty$, and $\Delta\bar{C}_p^\infty$. The curves for RT ln $w(T,7)$ and RT ln $w(T,2)$ are similar in general appearance and in range, raising the question whether some compromise algorithm exists which would satisfactorily encompass both data sets. We next discuss this point, first physically and then empirically.

The accepted picture of the physics underlying the intramolecular, interhelix interaction is given above: stability is provided by a combination of block-to-opposite-block hydrophobic and electrostatic interactions, both of which exist in full force at nearly neutral pH. At pH 2, however, the carboxylates are discharged and one must inquire as to the effect this might have. The effect on block-to-opposite-block hydrophobic interactions should be immaterial. On the other hand, the favorable block-to-opposite-block electrostatic interactions disappear at pH 2. One would therefore expect RT ln $w(T,2)$ to be less than RT ln $w(T,7)$ by just the contribution of the electrostatic free energy of the two salt bridges. Figure 5A shows that such a difference indeed exists from ~12 to 55 °C, where it amounts at most to only ~50 cal·mol^{-1}, but the reverse holds outside that range. This middle range includes virtually the entire meaningful range of the transition at near-neutral pH. Larger differences (opposite in sign) appear only at the extremes of the accessible temperature range, i.e., <12 °C, where RT ln $w(T)$ cannot be obtained, or >55 °C, where the only applicable CD data are for pH 2. These results therefore suggest (but only *suggest*) that salt bridges, while important in preventing antiparallel structures, contribute only ~10% of the total interhelix stabilization free energy near neutral pH. Since this is a rather small fraction, it reemphasizes that a combined algorithm might serve for both data sets.

It might be argued that this analysis is incomplete in that acidification of tropomyosin, in addition to the destruction of local interhelix electrostatic *attractions*, also increases the net charge, creating additional *repulsions*. However, we do not think this general electrostatic effect can be very important in the cases here considered, because

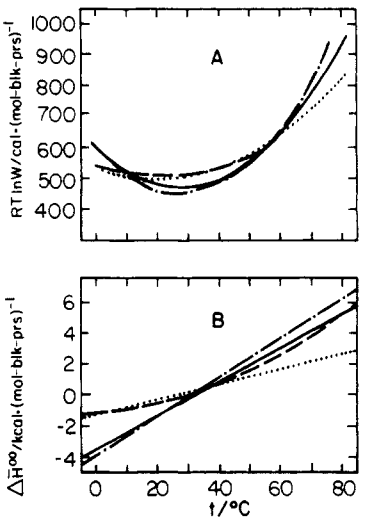

Figure 5. (A) Comparison of various algorithms for intramolecular, interhelix stabilization free energy: dotted curve, RT ln $w(T,7)$; dot–dash curve, RT ln $w(T,2)$; solid curve, RT ln $w(T,2ad)$; dashed curve, RT ln $w(T,7/2ad)$. (B) $\Delta\bar{H}^\infty$ curves corresponding to free energy curves in (A).

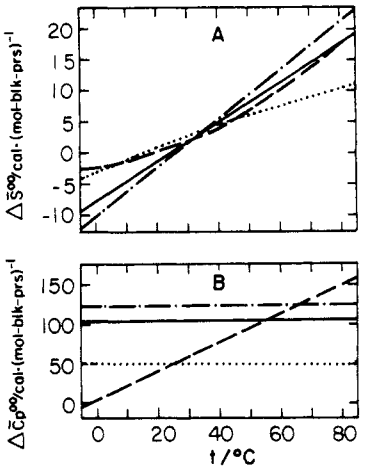

Figure 6. $\Delta\bar{S}^\infty$ (A) and $\Delta\bar{C}_p^\infty$ (B) curves corresponding to free energy curves in Figure 5A.

the ionic strength in both cases was over 0.5 M. In the vicinity of 0.5–1.0 M, the transition is very insensitive to ionic strength, leading us to the view that generalized electrostatic interactions are very well shielded and do not contribute greatly to the overall stability.

Since both superficial examination of Figure 5A and a qualitative look at the physics of interhelix interaction suggest the possibility of a reconciliation of the RT ln $w(T,7)$ and RT ln $w(T,2)$ algorithms, we next examine the possibility from the purely empirical point of view. As will be seen, this reconciliation is not in fact feasible.

The nature of the difficulty is exemplified on Figure 2B, whereon are plotted the points for fraction helix from CD at pH 2. The solid curves of that figure are values of fraction helix calculated for the two extreme protein concentrations using the RT ln $w(T,2)$ algorithm. Since these calculations also employ values of σ and $s(T)$ appropriate to the aspartic and glutamic acid residues at pH 2, we refer to these curves as $\Phi_h[\sigma(2),s(T,2),w(t,2)]$. As already noted, the calculations agree well with experiment. Also shown on Figure 2B (dotted curves) are curves of $\Phi_h[\sigma(2),s(T,2),w(T,7)]$, giving theoretical values of fraction helix at pH 2, but using the RT ln $w(T,7)$ interhelix algorithm, which was originally calculated to fit data near pH 7. The dotted curves are definitely unsatisfactory at the higher temperatures (>60 °C). They indicate much smaller helix content than the experiment. The difference, in fact, is not only quantitative but qualitative. The experiments require that, even at temperatures as high as 70 °C or more, the helix content not only remain high, but independent of concentration, forcing the inference that no appreciable chain dissociation occurs. On the other hand, the theory with RT ln $w(T,7)$ predicts marked chain dissociation above 60 °C, with concomitant concentration dependence and disastrous effect on the helix content.

At first we harbored the view that a "compromise" algorithm might avoid this disaster encountered by the RT ln $w(T,7)$ algorithm when it confronts the pH 2 data. However, only a few theoretical calculations are required to demonstrate that this is not possible. For such a combined algorithm to work, it must provide a value of RT ln $w(T)$ which, when applied to the highest protein concentration at pH 7.4 and 70 °C, yields a helix content of <15%; yet, when the same is applied to the lowest concentration at pH 2 and 70 °C, it must give a helix content >65%. Otherwise, one or the other data sets will not agree with theory. Our calculations show that to satisfy the first requirement necessitates a value of $w(70\ °C) \simeq 3.12$, but use of this value in the second (low pH) case provides a helix content of somewhat less than 40%, whereas the data are greater than 65%. The theory does not allow enough freedom to produce a satisfactory combined fit.

Since we cannot produce a combined fit, there is a distinct possibility that the interhelix stabilization free energy is simply different at pH 7.4 and at pH 2 for reasons that are yet to be clarified. Very little is in fact known about the details of these interactions. However, being understandably reluctant to relegate this important interaction to the unknown, we are impelled to consider another possibility. The problem, as has been seen, lies in the comparison of results at nearly neutral and at acidic pH in the high-temperature region. That comparison is, of course, only as good as the theory itself (which is already as good as we know how to make it), but also only as good as the CD data and the σ and $s(T)$ parameters employed to realize the theory. We are therefore led to the question whether some of the discrepancy might be due to relatively small errors in these input quantities. Our answer will be that this is also a distinct possibility; indeed, at present it is the possibility we most favor, although it is as yet unproven.

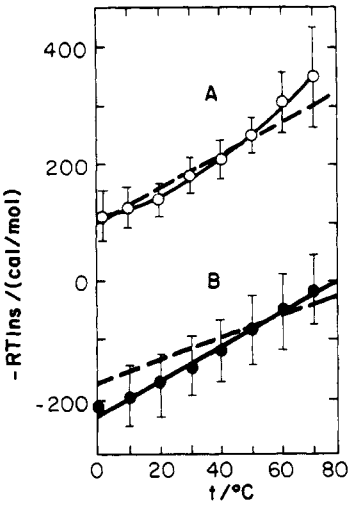

Figure 7. Plot of data from ref 35 and 28 on helix propagation free energies for aspartic (A) and glutamic (B) acid residues at pH 2. Error bars are from the same references. Solid line in each case is from ref 13, giving the "best" algorithm for the data. Dashed line in each case is the "adjusted" algorithm.

In conducting the inquiry, we focus on the values of $s(T)$ for glutamic and aspartic acids.[28,35] These represent the "worst case" and therefore are most likely to be the cause of the discrepancy for the following reasons: (1) Examination of the graphs of the original data shows that experimental errors are much larger for aspartic or glutamic acids than for aspartate or glutamate. (2) Experimental errors are also larger at high temperature, where the difficulty lies. Moreover, measurements of $s(T)$ do not extend beyond 70 °C; so the entire relevant range of temperatures is at the very upper end of the range of validity of the $s(T)$ algorithms. (3) Aspartic and glutamic acids are very common residues (glutamic is the most common); hence a small error in $s(T)$ for either residue has a substantial effect on helix content. (4) Glutamic acid, the most common residue, has $s(T) \approx 1.0$ in the high-temperature region. Near $s(T) \approx 1.0$, the conformation becomes very sensitive to the exact value of s.

Our aim, then, is to reexamine the data for $-RT$ ln $s(T)$ of aspartic and glutamic acids to see if these algorithms could be adjusted, within reasonable limits, in a manner that would allow both CD data sets to be satisfactorily fit with the same algorithm for RT ln $w(T)$. The original $-RT$ ln $s(T)$ data are replotted (after Figure 17 of ref 35 and Figure 10 of ref 28) on Figure 7 along with the experimental errors originally presented. The original algorithms through the data, as used here, are also shown (solid curves).[11] After some trial and error, we also drew a dashed line through the data for each of the two acidic residues as shown. These dashed lines represent the "adjusted" algorithm for each acidic residue and provide values we will refer to generally as $s(T,2ad)$. These "adjusted" lines are rather conservatively drawn in that they still pass through the error bars of all the points. Indeed, the aspartic acid line fits the data almost as well as the original algorithm. Moreover, the adjusted lines for both residues provide values of $\Delta\bar{H}°$ and $\Delta\bar{S}°$ that are within the experimental error (as given by the original authors[28,35]) of those given by the original algorithms.

These "adjusted" algorithms were used in the theory to fit the data at pH 2; the resulting values of RT ln $w(T,2ad)$ are displayed in Figure 8A. The best fit curve to these

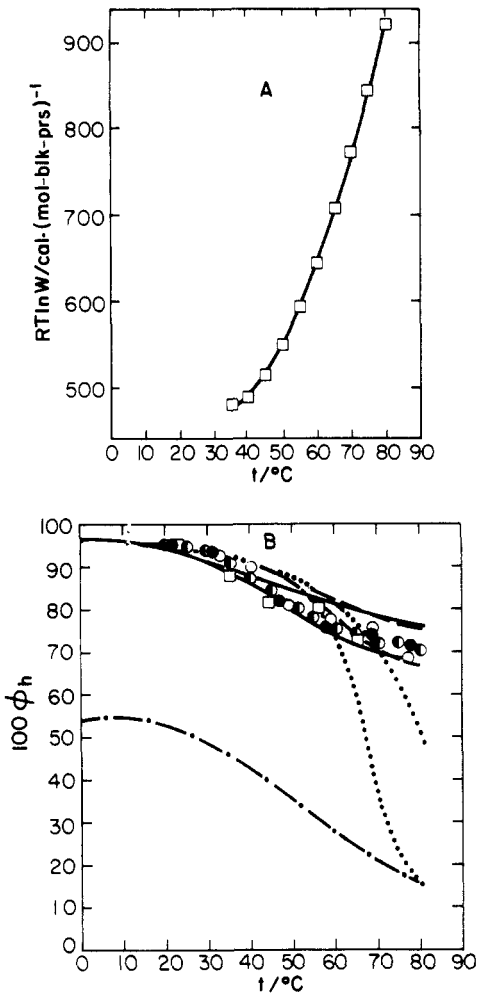

Figure 8. (A) RT ln w vs. temperature for non-cross-linked α-tropomyosin at pH 2: open squares, 0.0058 mg·cm^{-3}. Solid curve is RT ln $w(T,2ad)$ algorithm. (B) Percent helix vs. temperature for non-cross-linked α-tropomyosin at pH 2 with adjusted parameters for acidic residues. Data are same as in Figure 2B. Solid curves are from theory using RT ln $w(T,2ad)$ algorithm (i.e., curves give $\Phi_h[\sigma(2),s(T,2ad),w(T,2ad)]$ for 0.0058 (lower curve) and 5.2 (upper curve) mg·cm^{-3}. Dashed curves are from theory using RT ln $w(T,7/2ad)$ combined algorithm (i.e., curves give $\Phi_h[\sigma(2),s(T,2ad),w(T,7/2ad)]$) for same two concentrations. Dotted curves are from theory using RT ln $w(T,7)$ algorithm (i.e., curves give $\Phi_h[\sigma(2),s(T,2ad),w(T,7)]$) for same two concentrations. Dot–dash curve is from theory for single chains at pH 2 with adjusted $s(T)$ for acidic residues.

values is also shown on Figure 8A, the coefficients of the corresponding algorithm are given in Table I, and the algorithm is compared with previously discussed ones in Figure 5A (solid curve). That this RT ln $w(T,2ad)$ algorithm fits the low-pH data can be seen from the solid curves of Figure 8B. As in the case of the RT ln $w(T,2)$ algorithm, the theory predicts an immeasurably narrow range of helix content (for the range of protein concentrations employed), which brackets the data. The dotted and dot–dash curves on Figure 8B are analogous to those of Figure 2B except that those in Figure 8B were obtained by using the adjusted values of $s(T)$ for aspartic and glutamic acids. The dashed curve on Figure 8B will be discussed below.

So far, the "adjusted" values, while they provide just as good a fit as the original ones, have not been shown to produce any improvement in reconciling the algorithms from data at the two pH values. However, the combined plot of RT ln w values from data sets at both pH values, as given in Figure 9, now plainly suggests that a single algorithm might fit all the points. This combined algorithm, referred to as RT ln $w(T,7/2ad)$, is shown in Figure 9 and on Figure 5A (dashed curve) and its numerical coefficients are also given in Table I. That this combined algorithm fits the pH 7.4 data about as well as the original one does is seen from comparing Figure 10, wherein the dashed curves represent $\Phi_h[\sigma(7),s(T,7),w(T,7/2ad)]$, with Figure 2. That the combined algorithm also fits the pH 2 data is seen in Figure 8B, wherein the dashed curves, representing $\Phi_h[\sigma(2),s(T,2ad),w(T,7/2ad)]$, may be compared with the solid curves, representing $\Phi_h(\sigma(2),s(T,2ad),w(T,2ad)]$, as well as with the data. The fit to the cross-linkability data may also be judged satisfactory from Figure 4.

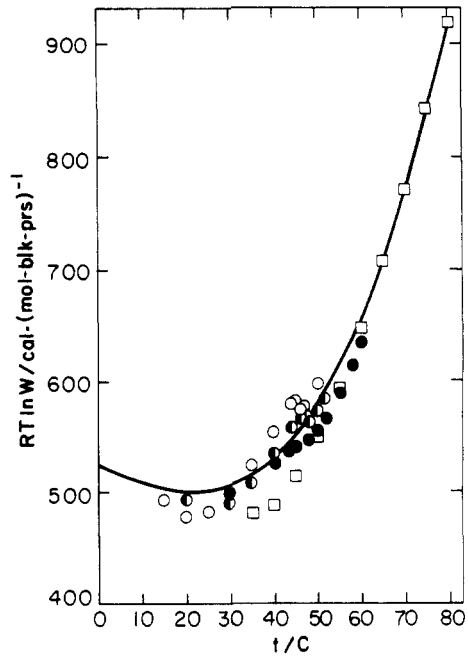

Figure 9. RT ln w vs. temperature for non-cross-linked α-tropomyosin at pH 7.4 and at pH 2 using adjusted algorithms for the latter. Circles are for pH 7.4 as in Figure 1A. Sqaures are for pH 2 as in Figure 8A. Solid curve is RT ln $w(T,7/2ad)$, the fit to the combined data set.

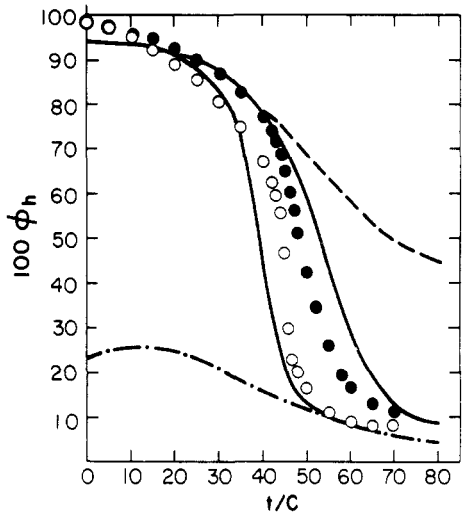

Figure 10. Percent helix vs. temperature for non-cross-linked α-tropomyosin at pH 7.4. Points are same smoothed data as in Figure 1B. Solid curves are from theory using RT ln $w(T,7/2ad)$ combined algorithm (i.e., curves are $\Phi_h[\sigma(7),s(T,7),w(T,7/2ad)]$). Dashed curve is from theory for dimer species using same algorithm. Dot–dash curve is from theory for single chains at pH 7.4.

These results indicate that rather conservative adjustments of the $s(T)$ values for aspartic and glutamic acids,

keeping within the experimental errors of the measurements, can result in a unifying algorithm for the interhelix interaction free energy that surely qualitatively, and perhaps even semiquantitatively, fits all the data we have. Thus, we certainly cannot rule out the possibility that the interhelix interaction is essentially pH independent. Indeed, we believe it to be the most likely of the possibilities confronting us.

V. Conclusions

The theory in its present form serves to rationalize all the known qualitative features of the tropomyosin thermal transition that do not depend upon local variations in intramolecular, interhelix interactions. Many of these features are semiquantitatively explained. At least one ($M_w(T)$ vs. T) was predicted theoretically before the experiment was performed. Some had previously resisted explanation. Some features are predicted by theory that have yet to be tested.

Among the known features that the theory renders intelligible are the following: (1) The thermal transition at near-neutral pH over a ~1000-fold range in protein concentration is semiquantitatively explained. The qualitative picture that emerges is that near neutral pH, dimer molecules maintain appreciable helix content to relatively high temperatures. The catastrophic loss of helix is primarily due to dissociation to single chains which are never (see (2) below) highly helical at pH 7. Thus, the observed dependence on protein concentration is explained by mass action. The molecular population at benign temperatures comprises only molecules close to in register. In the transition region, single chains coexist in equilibrium with a broad spectrum of dimer species including those more or less out of register. However, species containing randomly coiled loops, i.e., two-chain molecules containing two interacting helical stretches separated by a randomly coiled stretch on each chain, are essentially absent because of unfavorable loop entropy.

(2) It has long been recognized that in the absence of tertiary or quaternary interactions, single-chain protein helices are not manifest under ordinary conditions.[9] Theory renders this intelligible. Near pH 7, where the vast majority of experiments are done, single chains are never very helical at any temperature, even in tropomyosin, a protein almost fully helical in the native state. The short-range interactions do not provide enough stability near neutral pH.

(3) This picture explains the almost complete (~90%) cross-linkability of tropomyosin near room temperature. Theory predicts that the bulk of the molecules are near-register dimers under the conditions used in cross-linking. The theoretically predicted value for the fraction *exactly* in register is ~50%, somewhat less than the ~90% that is observed to cross-link. The remainder may easily be made up by small thermal fluctuations and/or thermally induced mobile equilibria between exactly registered molecules and those one or two heptets out of register. Theory predicts the overall fraction of molecules two heptets or less out of register to be ~90%. Furthermore, the present implementation of the theory postulates uniform interhelix interaction. Introduction of local variations in $RT \ln w(T)$ along the helices would likely serve to improve the predicted registration even further.

(4) Qualitatively, the chain dissociation predicted for the thermal transition near neutral pH in the original theory is also predicted in the augmented theory. Numerically, the difference is slight. The theoretical values agree within experimental error with the light scattering experiments. Chain dissociation and loss of helix are concurrent events. This view is by no means commonly held at present.

(5) The thermal transition at acidic pH has been something of a mystery for more than 20 years. Why should tropomyosin be so much more stable at low pH? Net charge is higher. Interchain salt linkages are gone. The theory renders this observation intelligible: Net charge is not very important at the high ionic strengths employed and interhelix interactions are rather similar at the two pH values, indicating that the salt linkages, while they may be sufficient to ensure parallelism, may not be more than 10% of the total stabilization free energy. The free energy of interhelix interaction is predominantly hydrophobic and independent of pH. The answer for augmented stability in acid thus lies mostly in the short-range $[\sigma,s(T)]$ interactions, which predict much higher helix content for single chains at pH 2 (see two lowest curves on Figure 2B). At pH 2, σ and $s(T)$ for Asp and Glu residues are enhanced; these constitute a sizable fraction (~28%) of the total number of residues. The resulting substantial helix content leads to a molecular population of almost exclusively two-chain molecules, explaining the lack of concentration dependence in the thermal transition at low pH.

In addition to explaining known facts, the theory also impels consideration and possibly further experimentation on some issues not raised before: (1) Theory requires interhelix stabilization in the range 500–800 cal/(mol of interacting block pairs)$^{-1}$. To our knowledge, no other estimate, experimental or theoretical, exists for this free energy, nor for the opinion, voiced here for reasons given above, that it is mostly hydrophobic in nature. In that vein, a question can be raised concerning chain parallelism in the equilibrium state, which is experimentally proven in the case of nearly neutral pH, but merely assumed in the case of acidic pH. It is worth pondering what might cause the two chains to arrange themselves exclusively in parallel, if indeed they do so, at low pH, where there can be no interhelix salt links. The crudest of estimates suggests that, at very high helix content, the contribution of charges at e and g positions to the free energy of stabilization of the parallel over the antiparallel structure is reduced by a factor of at least 4 if the carboxylates are discharged. (2) The putative mobile equilibrium among almost-registered coiled coils at benign temperatures raises questions concerning the possible mechanisms of such movements and experimental techniques that might detect them. (3) The temperature dependence of the interhelix interaction free energy is intriguing. If our interpretation is correct, one can read here, primarily, the temperature dependence of a hydrophobic interaction. Yet, the shape (i.e., the resulting $\Delta\bar{H}^\infty$, $\Delta\bar{S}^\infty$, $\Delta\bar{C}_p^\infty$; see Figures 5B, 6A, and 6B) is not reconcilable with the conventional wisdom concerning such interactions.[11]

At least two major questions have not yet been so much as addressed in our application of the augmented theory. First, there is the question of the influence of local variations in interhelix interaction. It seems well established that the amino terminal half of the molecule is more stable than the rest.[52] The difference lies in the interhelix interaction and is ~100 cal·(mol of interacting block pairs)$^{-1}$.[14] Although there is some disagreement, the preponderance of opinion is that the thermal transition, as seen in calorimetric,[49] fluorimetric,[53] and spin-label[54,55] experiments, occurs in at least two stages. Our implementation, using the uniform interaction model, necessarily obscures such detail. It remains to be seen whether the use of somewhat different interaction free energies for the two halves suffices to better mimic the behavior that has

been deduced from calorimetric and from labeling experiments. However, several things can be said at the outset about our physical, statistical picture of the transition, compared with the picture advanced by the laboratories in which the calorimetric and labeling data were obtained and elsewhere. According to the latter, the transition occurs in at least two,[53-55] some would say six,[49] stages. Each stage is supposed to involve a specific segment of the polypeptide chain and to be, in essence, an all-or-none transition. Only the final stage is accompanied by dissociation. This model seems to us, from the vantage point of helix–coil theory, extremely unlikely for a variety of reasons, some theoretical, some experimental, which deserve presentation.

First, it seems to us extremely unlikely that differences in interhelix interaction free energy (long-range interactions) in the two halves are huge; 100 cal·(mol of block pairs)$^{-1}$, the difference suggested earlier, represents only $\sim$20% of the total. It is clear, moreover, that the two halves differ very little in short-range interactions.[14] Statistical thermodynamics then simply insists that all species must coexist, although, of course, with somewhat modified populations. In such a system, there can be no all-or-none stages. Second, these models invariably yield some stage(s) in which the dimer molecule contains at least one appreciable segment of random coil lying between two, intact, double-helical segments, a species virtually forbidden by its enormous loop-entropic cost. Third, we point to the direct evidence from light scattering data that the onset of serious helix loss and of chain dissociation are concurrent. Fourth, we find it physically implausible that successive stages should involve unfolding of a double-helical segment while its neighbor remains intact, followed by unfolding of the second segment accompanied by *refolding* of the first.[49]

Fifth, and finally, we take issue with the interpretation of the spin-label data that has given rise to the all-or-none-stages model. Both earlier[54] and more recent[55] spin label experiments have been interpreted in this manner. The earlier work was done in this laboratory. However, the later work reveals that exposure to above-neutral pH causes a subsequent chemical reaction of the spin label (label species I) with the protein that results in species in which one end of the maleimide label is linked covalently to the sulfhydryl target and the other to a vicinal side-chain lysine amino (to form label species II). The earlier work, it now appears, was done, willy-nilly, with label species II. In the later work, it was shown by CD that tropomyosin bearing label species II denatures differently from tropomyosin itself, displaying a prominent "pretransition" which is also clearly seen in both spin label studies. Tropomyosin bearing label species I, on the other hand, shows a CD transition indistinguishable from that of tropomyosin itself and shows a spin transition that shows no pretransition.

Contrary to the authors of ref 55, we feel that the most likely explanation of these facts is that (a) in tropomyosin and in tropomyosin labeled with species I, there simply is no pretransition and (b) in tropomyosin labeled with species II, the label-formed covalent loop from Cys-190 to Lys-189 dramatically alters the local helix stability. This specter of a label that may merely report on behavior it itself has induced was raised previously.[54] The statistical mechanical model advanced here and the all-or-none-stages model are very different, and it will remain for future work to produce convergence to a correct picture. In our opinion, the all-or-none stages model not only is disfavored by all but the calorimetric experimental evidence but is, because it reckons without loop entropy, nonphysical. These difficulties remain to be reconciled.

The second question that our application of the augmented theory has not yet addressed is that of the thermal transition in dimer molecules that have been cross-linked at Cys-190. Sufficient experimental data exist to make such comparisons, and, indeed, in earlier applications of the more limited theory, comparisons of these data with calculations of the helix content of the two-chain species played a prominent role.[11-13] However, a more recent and much deeper theoretical analysis of the populations of states characterizing systems of such tethered molecules[56] has convinced us that our initial, intuitive identification of these molecules with non-cross-linked dimers is superficial and perhaps seriously in error. A separate theoretical framework is required to treat the cross-linked case. We hope to address the problem in the near future.

Acknowledgment. This study was supported in part by Grant No. GM-20064 from the Division of General Medical Sciences, U.S. Public Health Service, and in part by the Biophysical Program of the National Science Foundation, Grant No. PCM-83-43209.

References and Notes

(1) Fraser, R.; MacRae, T. "Conformation in Fibrous Proteins"; Academic Press: New York, 1973; pp 419–468.
(2) Cohen, C.; Szent-Györgyi, A. G. *J. Am. Chem. Soc.* **1957**, *79*, 248.
(3) Holtzer, A.; Clark, R.; Lowey, S. *Biochemistry* **1965**, *4*, 2401–2411.
(4) Woods, E. *Biochemistry* **1969**, *8*, 4336–4344.
(5) Caspar, D.; Cohen, C.; Longley, W. *J. Mol. Biol.* **1969**, *41*, 87–107.
(6) Johnson, P.; Smillie, L. *Biochem. Biophys. Res. Commun.* **1975**, *64*, 1316–1322.
(7) Lehrer, S. *Proc. Natl. Acad. Sci. U.S.A.* **1975**, *72*, 3377–3381.
(8) Stewart, M. *FEBS Lett.* **1975**, *53*, 5–7.
(9) Talbot, J.; Hodges, R. *Acc. Chem. Res.* **1982**, *15*, 224–230.
(10) Skolnick, J.; Holtzer, A. *Macromolecules* **1982**, *15*, 303–314.
(11) Skolnick, J.; Holtzer, A. *Macromolecules* **1982**, *15*, 812–821.
(12) Holtzer, M. E.; Holtzer, A.; Skolnick, J. *Macromolecules* **1983**, *16*, 173–180.
(13) Holtzer, M. E.; Holtzer, A.; Skolnick, J. *Macromolecules* **1983**, *16*, 462–465.
(14) Skolnick, J.; Holtzer, A. *Macromolecules* **1983**, *16*, 1548–1550.
(15) Hodges, R.; Sodek, J.; Smillie, L.; Jurasek, L. *Cold Spring Harbor Symp. Quant. Biol.* **1972**, *37*, 299–310.
(16) Mak, A.; Smillie, L.; Stewart, G. *J. Biol. Chem.* **1980**, *255*, 3647–3655.
(17) Mak, A.; Lewis, W.; Smillie, L. *FEBS Lett.* **1979**, *105*, 232–234.
(18) McLachlan, A.; Stewart, M. *J. Mol. Biol.* **1975**, *98*, 293–304.
(19) Parry, D. *J. Mol. Biol.* **1975**, *98*, 519–535.
(20) Zimm, B.; Bragg, J. *J. Chem. Phys.* **1959**, *31*, 526–535.
(21) Nagai, K. *J. Phys. Soc. Jpn.* **1960**, *15*, 407.
(22) Poland, D.; Scheraga, H. "Theory of Helix–Coil Transitions in Biopolymers"; Academic Press: New York, 1970.
(23) Ananthanarayanan, V. S.; Andreatta, R. H.; Poland, D.; Scheraga, H. A. *Macromolecules* **1971**, *4*, 417.
(24) Platzer, K. E. B.; Ananthanarayanan, V. S.; Andreatta, R. H.; Scheraga, H. A. *Macromolecules* **1972**, *5*, 177.
(25) Alter, J. E.; Taylor, G. T.; Scheraga, H. A. *Macromolecules* **1972**, *5*, 539.
(26) Van Wart, H. E.; Taylor, G. T.; Scheraga, H. A. *Macromolecules* **1973**, *6*, 266.
(27) Alter, J. E.; Andreatta, R. H.; Taylor, G. T.; Scheraga, H. A. *Macromolecules* **1973**, *6*, 564.
(28) Maxfield, F. R.; Alter, J. E.; Taylor, G. T.; Scheraga, H. A. *Macromolecules* **1975**, *8*, 479.
(29) Schuele, R. K.; Cardinaux, F.; Taylor, G. T.; Scheraga, H. A. *Macromolecules* **1976**, *9*, 23.
(30) Dygert, M. K.; Taylor, G. T.; Cardinaux, F.; Scheraga, H. A. *Macromolecules* **1976**, *9*, 794.
(31) Matheson, R. R.; Nemenoff, R. A.; Cardinaux, F.; Scheraga, H. A. *Biopolymers* **1977**, *16*, 1567.
(32) van Nispen, J. W.; Hill, D. J.; Scheraga, H. A. *Biopolymers* **1977**, *16*, 1587.
(33) Hill, D. J.; Cardinaux, F.; Scheraga, H. A. *Biopolymers* **1977**, *16*, 2447.
(34) Konishi, Y.; van Nispen, J. W.; Davenport, G.; Scheraga, H. A. *Macromolecules* **1977**, *10*, 1264.

(35) Kobayashi, Y.; Cardinaux, F.; Zweifel, B. O.; Scheraga, H. A. *Macromolecules* **1977**, *10*, 1271.
(36) Hecht, M. H.; Zweifel, B. O.; Scheraga, H. A. *Macromolecules* **1978**, *11*, 545.
(37) Fredrickson, R.; Chang, M.; Powers, S.; Scheraga, H. *Macromolecules* **1981**, *14*, 625–632.
(38) Denton, J.; Powers, S.; Zweifel, B.; Scheraga, H. *Biopolymers* **1982**, *21*, 51–77.
(39) Skolnick, J. *Macromolecules* **1983**, *16*, 1069–1083.
(40) Skolnick, J. *Macromolecules* **1983**, *16*, 1763–1770.
(41) Skolnick, J. *Macromolecules* **1984**, *17*, 645–658.
(42) Isom, L.; Holtzer, M. E.; Holtzer, A. *Macromolecules* **1984**, *17*, 2445–2447.
(43) Yukioka, S.; Noda, I.; Nagasawa, M.; Holtzer, M. E.; Holtzer, A. *Macromolecules*, in press.
(44) Mayer, J.; Mayer, M. "Statistical Mechanics"; Wiley: New York, 1940; pp 215–217.
(45) Zimm, B. *J. Chem. Phys.* **1960**, *33*, 1349.
(46) Chou, K.-C.; Nemethy, G.; Scheraga, H. *J. Phys. Chem.* **1983**, *87*, 2869–2881.
(47) Phillips, G. *Biophys. J.* **1984**, *45*, 392a.
(48) Tsong, T.; Himmelfarb, S.; Harrington, W. *J. Mol. Biol.* **1983**, *164*, 431–450.
(49) Potekhin, S.; Privalov, P. *J. Mol. Biol.* **1982**, *159*, 519–535.
(50) It is likely that cross-linking is even faster, requiring, at most, minutes rather than hours. This conclusion is based on unpublished work by Dr. M. E. Holtzer, who finds that tropomyosin in sodium dodecyl sulfate, where the chains are separate, has all its sulfhydryls blocked by $(NbS)_2$ in <10 min. At that rate, $(NbS)_2$ could only cross-link as well as it does in benign media if the reaction of a reacted (blocked) sulfhydryl with its still unblocked neighbor is faster still. Otherwise, both neighboring sulfhydryls would be blocked before any cross-links could form.
(51) Holtzer, M. E.; Breiner, T.; Holtzer, A. *Biopolymers* **1984**, *23*, 1811–1833.
(52) Pato, M.; Mak, A.; Smillie, L. *J. Biol. Chem.* **1981**, *256*, 593–601.
(53) Betteridge, D.; Lehrer, S. *J. Mol. Biol.* **1983**, *167*, 481–496.
(54) Chao, Y.-Y.; Holtzer, A. *Biochemistry* **1975**, *14*, 2164–2170.
(55) Graceffa, P.; Lehrer, S. *Biochemistry* **1984**, *23*, 2606–2612.
(56) Skolnick, J., unpublished work.

Solvent Effects and Initiation Mechanisms for Graft Polymerization on Pine Lignin

John J. Meister* and Damodar R. Patil

Department of Chemistry, Southern Methodist University, Dallas, Texas 75275.
Received January 15, 1985

ABSTRACT: Graft copolymerization of 2-propenamide onto Kraft pine lignin, previously initiated with hydrogen peroxide and 3,3-dimethyl-1,2-dioxabutane, can be initiated with 2-hydroperoxy-1,4-dioxacyclohexane, an autoxidation product of 1,4-dioxacyclohexane. Graft copolymer is formed by free radical polymerization in dimethyl sulfoxide containing lignin, calcium chloride, and cerium(IV) ion. Initiation mechanisms based on hydroperoxide reaction with cerium(IV) or chloride ion were tested. The cerium ion/hydroperoxide mechanism does not explain the results of a series of test reactions. However, direct reaction of chloride ion and hydroperoxide did not occur and while chloride ion content of the reaction did correlate with product properties, so did chloride:hydroperoxide mole ratio and lignin:chloride mole ratio. This implies an initiation process involving chloride ion, hydroperoxide, and lignin may produce grafting.

Introduction

Every year the U.S. paper industry produces over 33 million metric tons of Kraft lignin.[1] Most of this biomass is burned as fuel but small amounts are used as binders, asphalt additives, or cement additives. Larger fractions of this waste would be used in other industrial or commercial processes if an economical way existed to convert lignin into a product useful for something more than a fuel.

A possible way to make such a conversion has now been produced.[2,3] The transformation converts Kraft pine lignin to a water-soluble copolymer by graft polymerization. Graft copolymer is formed by conducting a free-radical polymerization of 2-propenamide in nitrogen-saturated, 1,4-dioxacyclohexane containing lignin, calcium chloride, cerium (IV) ion, and 1,4-dioxacyclohexane autoxidation products. Further studies on this reaction have shown that improvements in the reaction process, product solubility, and product physical properties are possible by changing the solvent for the reaction. Further, a mechanism for initiation can now be postulated based on further studies of reaction and products.

Previously prepared graft copolymers have been made by producing 1,4-dioxacyclohexane autoxidation products directly in pure solvent and using autoxidation products without isolation. In this work, we show that the critical autoxidation product, 2-hydroperoxy-1,4-dioxacyclohexane, can be isolated, purified, and used to initiate this grafting reaction in other solvents.

We have also performed further tests to determine the relationship between product properties and reaction conditions. In the following sections, the synthesis procedure, product solubility properties, use of other solvents, possible mechanisms of initiation, mechanism tests, and syntheses run to define how product properties vary as a function of synthesis conditions will be described.

Experimental Section

In the graft polymer synthesis, oxidized 1,4-dioxacyclohexane is vacuum-distilled to separate 1,4-dioxacyclohexane and its autoxidation products. Autoxidation products are then purified and/or used directly to initiate the grafting reaction in another solvent.

Synthesis. To prepare 2-hydroperoxy-1,4-dioxacyclohexane, the time required to produce a maximum concentration of oxidizing equivalents in 1,4-dioxacyclohexane must be determined. Autoxidation is conducted by refluxing 250 mL of freshly distilled 1,4-dioxacyclohexane while bubbling the contents of the reflux vessel with air at a rate of 4.3 mL/s. Optimum duration for this treatment must be determined by conducting an iodine/thiosulfate titration on aliquots of solvent reflux and bubbled for different times.

After 1,4-dioxacyclohexane (I) is refluxed and aerated for the optimum time, unreacted I is removed at 0.27-kPa nitrogen pressure and 23 °C temperature. The isolated white solid is stored at 4 °C in a refrigerator. It is purified by saturating an equal volume mixture of hexane and 3-oxy-2-oxopentane with the solid and chilling to 0 °C. Precipitate is separated from supernate by cold filtration and the purified 2-hydroperoxy-1,4-dioxacyclohexane is stored at 4 °C.

The grafting reaction is run by adding lignin and calcium chloride to a nitrogen-flushed 125-mL flask containing 20 mL of solvent. The mixture is bubbled with nitrogen for 3 min, oxidation

0024-9297/85/2218-1559$01.50/0 © 1985 American Chemical Society